International Journal for Multidisciplinary Research (IJFMR)
E-ISSN: 2582-2160 ● Website: www.ijfmr.com ● Email: editor@ijfmr.com

Flow Simulation and Thrust Analysis of Solid Rocket Motor Using CFD

A.Varun Sai[1], Drakshi Mishra[2], Vinek Kumar Patil[3], Dr.Md.Fakruddin H.N.[4]

[1,2,3]Student, Mechanical Engineering Department, Methodist College Of Engineering And Technology,
[4]Professor, Mechanical Engineering Department, Methodist College Of Engineering And Technology.

Abstract

Solid Rocket Motors (SRMs) are widely used in aerospace applications due to their simplicity and high thrust output. However, traditional analytical methods often rely on ideal assumptions that fail to capture real internal flow dynamics, especially during propellant burnback. This study presents a CFD-based approach to simulate and analyze the internal flow and thrust performance of an SRM with a tubular grain configuration.

A two-dimensional axisymmetric model was developed, including the combustion chamber and a convergent-divergent nozzle. The grain length was initially set to 0.1 m and progressively reduced in steps of 0.01 m to simulate burnback. Each geometry was meshed using Pointwise, and steady-state simulations were carried out in ANSYS Fluent, considering compressible and turbulent flow.

The study concludes that CFD offers a reliable and detailed method for predicting SRM performance across varying burn stages. This approach overcomes the limitations of traditional 1D models and provides valuable insights for design and optimization in early-stage development.

Keywords: Solid Rocket Motor (SRM), Computational Fluid Dynamics (CFD), Grain Regression, Convergent-Divergent Nozzle, Isentropic Flow Analysis, Propellant Burnback, Tubular Grain

1. Introduction

Solid rocket motors (SRMs) have been an essential component of propulsion systems in both space and defense industries for decades, favored for their structural simplicity, high thrust output, and storability. However, despite their widespread application, the internal flow characteristics within SRMs remain complex and not completely understood. Traditional design and analysis techniques largely rely on idealized one-dimensional models and empirical correlations. These methods often fail to capture real-time variations in flow parameters, especially during transient phases of operation such as ignition, burning, and burnout. As a result, discrepancies between theoretical predictions and actual performance are not uncommon.

One of the most significant limitations in conventional SRM design methodology is the reliance on quasi-one-dimensional isentropic flow assumptions. While these equations provide a basic framework for calculating parameters like Mach number, pressure ratios, and thrust, they ignore key physical phenomena such as boundary layer growth, flow separation, turbulence, and heat transfer. These effects become particularly significant in the combustion chamber and nozzle throat regions, where high-speed

compressible flow interacts with solid surfaces. In addition, these methods often assume uniform flow distribution, neglecting the multi-dimensional nature of flow evolution within the chamber and nozzle. This oversimplification can lead to inaccurate estimations of thrust, pressure losses, and combustion stability.

Another issue with existing methods is the inability to simulate the grain regression process realistically. Most traditional studies assume a fixed grain geometry or average out the burning behavior over time. This approach is limited in its ability to predict transient performance parameters like thrust decay, chamber pressure variation, or nozzle flow transition throughout the burn time. Since the performance of an SRM is inherently dependent on how the propellant regresses and exposes burning surfaces, the lack of real-time simulation limits the ability of engineers to optimize grain design or evaluate burnout characteristics. Moreover, physical experiments that could address these limitations are costly, time-consuming, and often limited by safety and resource constraints.

To overcome these limitations, researchers have increasingly turned toward Computational Fluid Dynamics (CFD) as a tool to simulate the internal environment of SRMs. While there are many studies on nozzle flow simulations, many still focus on simplified geometries or isolated components, such as simulating just the nozzle or a section of the combustion chamber. The lack of a holistic simulation encompassing both the combustion chamber and nozzle in a coupled model with time-varying grain size remains a critical gap. Furthermore, in many previous works, validation is either neglected or performed against analytical models that assume ideal conditions, creating a feedback loop of approximation without anchoring the data in realistic physical behavior.

To address these issues, this study proposes a comprehensive CFD-based simulation framework for a solid rocket motor, which not only includes both the convergent-divergent nozzle and the combustion chamber but also incorporates realistic grain regression modeling. The simulation starts with an initial grain length of 0.1 m and reduces it gradually in steps of 0.01 mm until complete burnout is achieved. At each step, the geometry is updated, and flow simulations are performed using ANSYS Fluent, with the meshing done in Pointwise to ensure high precision. This method enables the continuous monitoring of changes in internal flow conditions and performance metrics like thrust, chamber pressure, Mach number, and temperature distribution as the grain size depletes.

By adopting this iterative and dynamic simulation approach, the project captures the transient behavior of SRMs more effectively than traditional static models. One of the key advantages of this approach is its ability to replicate the progressive thrust decay seen in real-world solid motors as the surface area for combustion decreases. Unlike ideal isentropic calculations that assume constant input parameters, the proposed CFD method accounts for fluid-structure interaction, viscous effects, and boundary layer development. These features make it possible to visualize how the flow evolves spatially and temporally within the rocket motor, offering insights that can inform design improvements and efficiency optimization.

Additionally, the simulation results are validated by comparing the Mach number and flow parameters at various sections of the nozzle with values obtained from an isentropic aerodynamic calculator. This dual validation method—using both theoretical data and simulation—ensures that the results are not only realistic but also quantitatively sound. The observed deviations between the simulation and theoretical predictions are expected due to the real-fluid effects captured by CFD, and they provide further confidence in the robustness of the model. The simulation also reveals flow phenomena such as shock wave formation, expansion waves, and nozzle choking conditions that are not evident in one-dimensional models.

In summary, the proposed method significantly improves upon existing SRM modeling techniques by integrating a realistic, time-dependent simulation of both combustion chamber and nozzle performance. It enables a more accurate estimation of thrust, offers better visualization of flow features, and helps identify inefficiencies in design. The use of modern CFD tools in this project demonstrates their potential as a powerful supplement or even replacement for traditional analytical and experimental approaches in the early design and performance evaluation stages of solid rocket motors.

2. Methodologies

The flow simulation study of the solid rocket motor (SRM) was carried out using Computational Fluid Dynamics (CFD) techniques to analyze the performance characteristics of the motor under varying internal grain configurations. The methodology comprises the creation of the SRM geometry, meshing for computational analysis, simulation setup using ANSYS Fluent, and a stepwise simulation process for varying grain sizes to reflect the progressive burnback of the solid propellant.

2.1 Geometry Design

The initial phase involved designing a two-dimensional axisymmetric model of the SRM, comprising a combustion chamber and a convergent-divergent nozzle. The geometry of the nozzle was generated using coordinates derived from standard nozzle contour equations. For the combustion chamber, a tubular grain design was adopted.

Internal diameter of grain	0.25m
External diameter of grain	0.125m
Thorat diameter	0.03m
Exit diameter	0.09m
Radius of convergent section	0.03m
Divergent angle	15
Grain length	0.6m

Table 1: Dimensions of solid rocket motor

Figure 1: Geometry of solid rocket motor

2.2 Mesh Generation

A structured quadrilateral mesh was performed using Pointwise software as shown in Figure 2, which allowed for the creation of a structured and refined mesh suitable for compressible flow analysis. Special attention was given to the throat and nozzle regions to capture high-gradient flow parameters accurately. The mesh was validated to ensure that it was grid-independent and optimized for simulation stability.

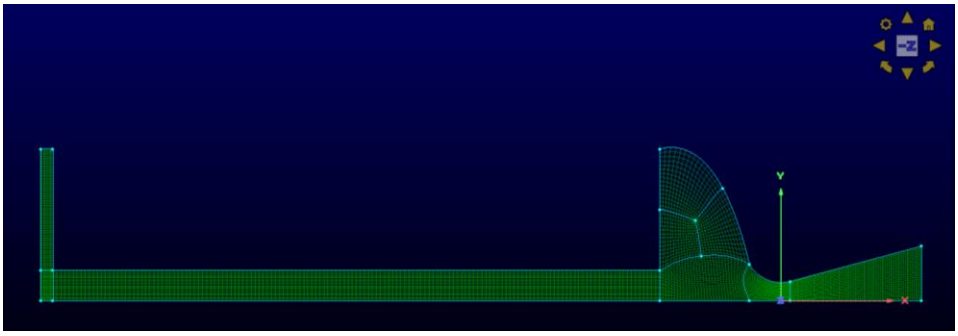

Figure 2: Geometry of solid rocket motor meshed in pointwise software

2.3 Simulation Setup

The simulation process was carried out using ANSYS Fluent, with the solver set to pressure-based and the flow modeled as compressible and turbulent. The working fluid was considered to be air, with standard atmospheric conditions set at the nozzle exit. The energy equation was enabled, and the k-ε turbulence model was used for capturing the flow characteristics inside the chamber and nozzle. Boundary conditions included pressure inlet for the chamber and pressure outlet at the nozzle exit. Wall conditions were set as adiabatic and no-slip.

Materials

Property	Air
Density	Ideal gas
Viscosity	Sutherland
Temperature	3000K

Table 2: material properties

Boundary conditions

Following boundary conditions were used

Initial Gauge Pressure	5MPa
Inlet Temperature	3000K
Outlet Pressure	1.3MPa
Outlet Temperature	300K

Table 3: Boundary conditions

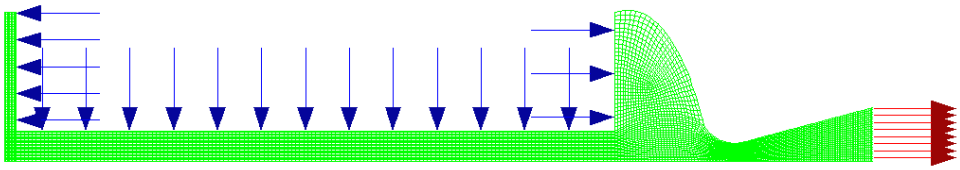

Figure 3: Simulation set up in ANSYS fluent

2.4 Grain Regression Study

To simulate the burnback behavior of the solid propellant, the grain length was progressively reduced in steps of 0.01m, starting from an initial length of 0.1 m and ending when the grain was fully depleted. At

each stage, the geometry was updated, and a new simulation was run to capture the corresponding changes in flow parameters and thrust.

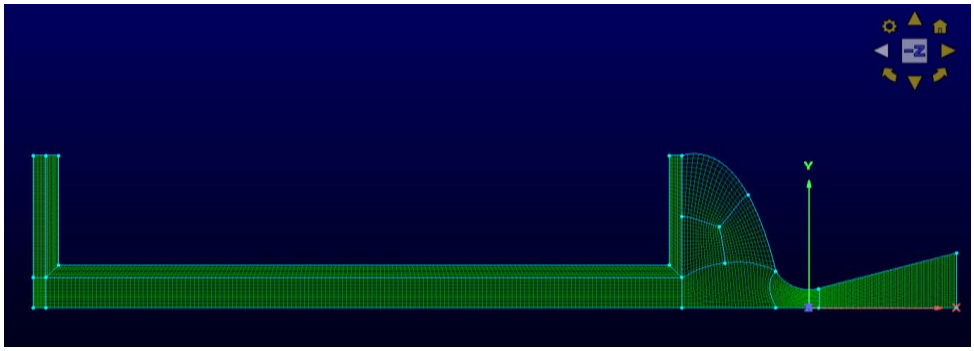

Figure 4: Initial 0.01m grain depth

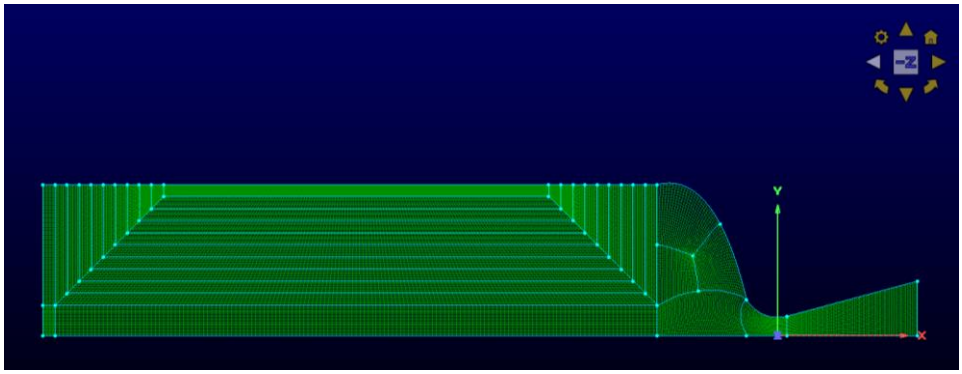

Figure 5: Final 0.1m grain depth or total burnout

2.5 Data Extraction and Analysis

For each simulation, thrust was calculated using the momentum equation at the nozzle exit. Mach number, pressure distribution, velocity profiles, and temperature fields were recorded and visualized using contour plots. XY plots were also generated to observe the trend of thrust with respect to grain size. These outputs were later compared with theoretical values calculated using an isentropic aerodynamic calculator to validate the simulation accuracy.

Equations

Thrust:

The force generated by the rocket due to the expulsion of high-speed gases.

Where,

$$T = \dot{m}v_e + (P_e - P_a)A_e \quad (1)$$

T = Thrust (N)

$\dot{m}$ = Mass flow rate of exhaust gases (kg/s)

v_e = Exit velocity of exhaust gases (m/s)

P_e = Exit pressure (Pa)

P_a = Ambient pressure (Pa)

A_e = Nozzle exit area (m^2)

Specific Impulse:

Measure's propellant efficiency, indicating how much thrust is produced per unit of propellant consumed.

$$I_{sp} = \frac{T}{\dot{m}g} \quad (2)$$

I_{sp}= Specific impulse (s)

g = Gravitational acceleration (9.81 m/s²)

Total Impulse:

The total thrust delivered over the burn duration:

$$I_T = \int T \, dt \quad (3)$$

3. Results and Discussion

The flow simulation results for the solid rocket motor (SRM) provided detailed insights into the internal flow behavior, performance characteristics, and the effect of grain regression on thrust output. A series of CFD simulations were conducted for various grain lengths ranging from 0.1 m to 0 m, decreasing in steps of 0.01 m, to mimic the burnback process of the solid propellant during operation.

3.1 Mach Number and Flow Distribution

Contour plots of Mach number shown in Figure 6 revealed a consistent transition from subsonic to supersonic flow through the nozzle's convergent-divergent profile. At full grain size, the flow achieved supersonic speeds just past the throat, with a Mach number exceeding 2.0 in the divergent section. As the grain regressed, although the inlet mass flow rate decreased, the flow continued to accelerate through the nozzle due to the pressure difference, though with slightly lower Mach values toward the end of the burn.

Figure 6: Contour of Mach number showing change of flow from subsonic to supersonic.

3.2 Pressure and Temperature Fields

Pressure distribution contour shown Figure 7 indicating high static pressure in the combustion chamber, gradually dropping through the nozzle, consistent with theoretical flow behavior. The highest chamber pressure was recorded during the initial phase with the full grain, and it decreased progressively with each step of grain regression. Temperature contours shown Figure 8 also followed a similar trend, showing peak values near the chamber inlet and throat area and cooling toward the nozzle exit.

Figure 7: Contour of static pressure showing the pressure drop at the throat

Figure 8: Contour showing decreasing of temperature at the outlet

3.3 Graphical Analysis

XY plots were generated to compare thrust, Mach number, and pressure for each grain size configuration. These plots highlighted the influence of grain geometry on the SRM's performance, validating the importance of time-dependent grain regression modeling in predicting realistic motor behavior.

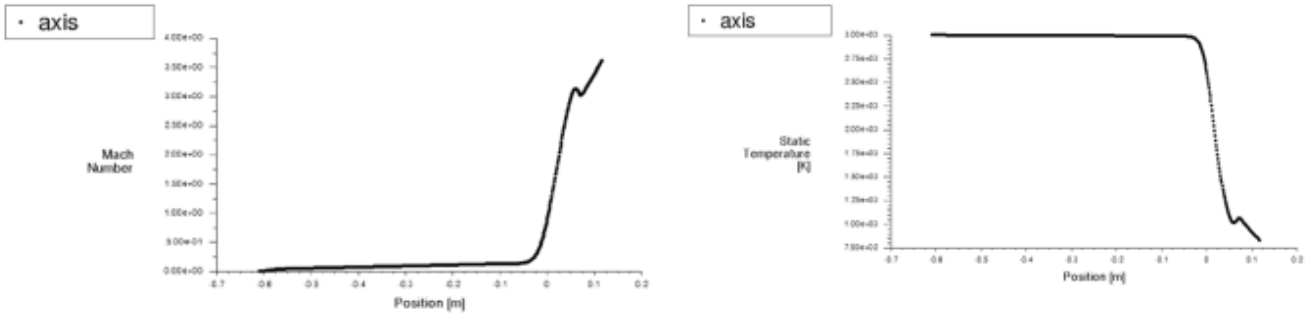

Figure 9: XY Plots showing increase in Mach number along axis and increase in temperature along the axis

Table Of Comparisons Of All Grain Size From 0.1m – 0m

S.no	Grain size	Mass flow rate ($\dot{m}$)	Pressure (P_e)	Velocity (v_e)	Volume (v)	Mass m_{Pro}	Thrust (T)	Specific impulse (I_{sp})	Total impulse (I_T)
	(m)	kg/sec	Pa	m/sec	m^3	kg	KN	sec	$KN-sec$
1	0.1	2.73	61211.1	2084.81	0.02827	49.75	5.436	202.97	99.07
2	0.09	3.29	71383.4	2088.89	0.02623	46.164	6.682	207.03	93.760
3	0.08	3.76	76287.5	2088.67	0.02392	42.099	7.694	208.59	86.146
4	0.07	4.45	87049.6	2084.65	0.02137	37.611	9.271	212.37	78.690
5	0.06	4.59	95004.9	2089	0.01862	32.771	9.548	212.04	68.167
6	0.05	4.88	101929	2088.28	0.01570	27.632	10.194	212.93	57.721
7	0.04	5.19	120707	2086.33	0.01266	22.281	10.951	215.08	47.013
8	0.03	5.22	115313	2080.4	0.00953	16.772	10.952	213.87	35.184
9	0.02	5.11	112987	2086.3	0.00335	5.896	10.735	214.14	27.386
10	0.01	5.14	107928	2086.26	0.00316	5.561	10.765	213.49	20.646
11	0.0	5.05	111602	2086.28	0	0	10.601	213.98	0

Table 4: Represents the thrust variation with grain burn back

1. Mass Flow Rate ($\dot{m}$) Increases

- As the grain size decreases, the mass flow rate increases, reaching its peak around 0.03m before slightly fluctuating.
- This is expected since more surface area burns per unit time as the grain burns back.

2. Thrust (T) Variation

- Initially, the thrust increases with decreasing grain size, peaking at around 0.03m (10.952 KN).
- After that, thrust starts to decrease as the available burning surface reduces further.
- When the grain size reaches zero, the thrust also becomes zero, indicating the complete burnout of the propellant.

The above data is pictured in next graphs

THRUST VS GRAIN SIZE

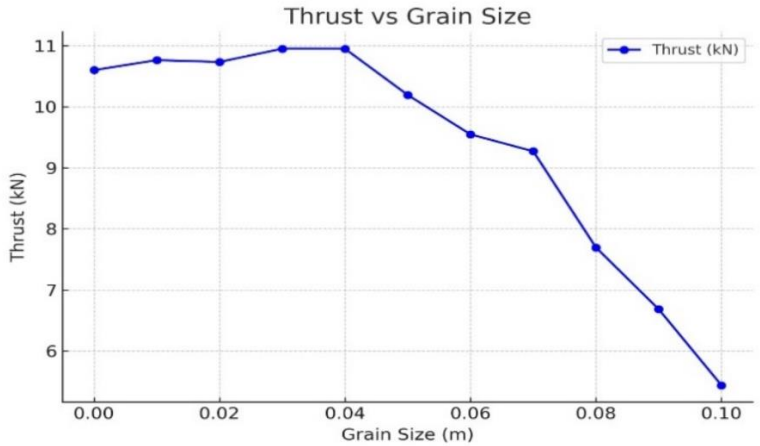

Figure 9: Thrust vs Grain Size: Shows how thrust varies with different grain sizes.

MASS FLOW RATE VS GRAIN SIZE

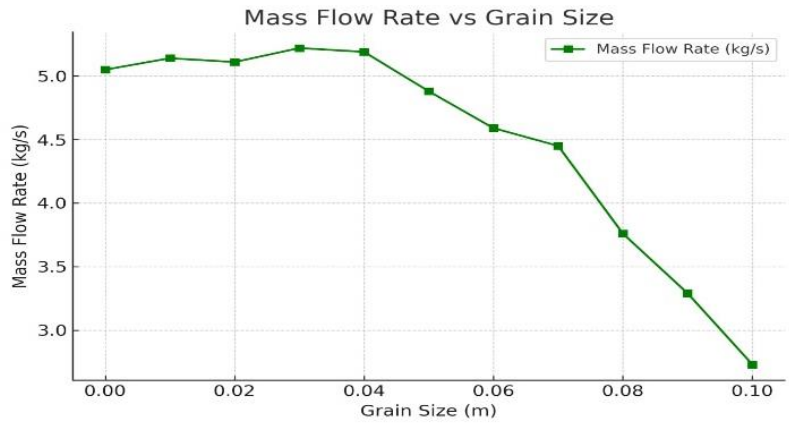

Figure 10: Mass Flow Rate Vs Grain Size: Indicates the Variation of Mass Flow Rate as the Grain Burns.

TOTAL IMPULSE VS GRAIN SIZE

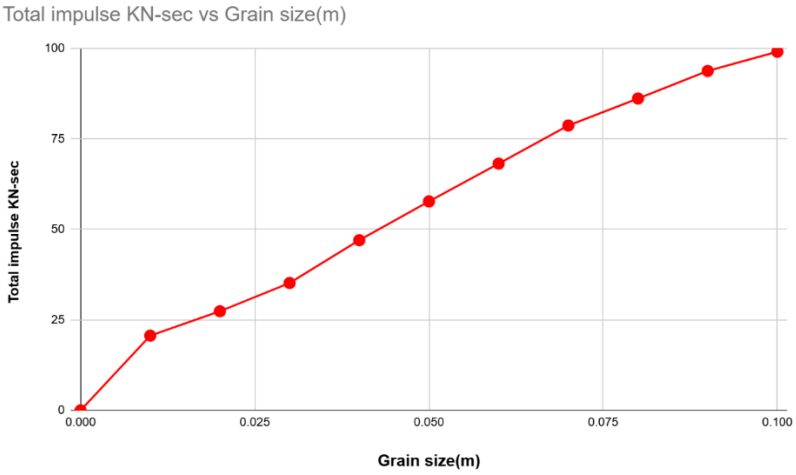

Figure 11: Total impulse vs grain size: displays how total impulse changes as the grain size reduces.

RESULT

The results obtained from the flow simulations of the solid rocket motor (SRM) provide insights into the performance of different grain sizes, the corresponding thrust, and overall motor efficiency.

The Observations Are:

Thrust Variation with Grain Size: As the grain size decreases, the thrust produced by the motor changes significantly. Initially, at a grain size of 0.1m, the thrust was 5.436 KN, and it increased as the grain burned until reaching a peak, before gradually decreasing when the grain size approached zero.

Mass Flow Rate Trends: The mass flow rate increased as the grain size decreased, peaking towards the final stages of combustion.

Velocity and Pressure Contours: The velocity contours showed high-speed exhaust gases exiting the nozzle, confirming efficient nozzle performance. The pressure distribution followed expected trends, with a high-pressure region in the combustion chamber and gradual expansion in the nozzle.

Total Impulse Calculation: The total impulse was calculated for each case, providing a cumulative measure of the rocket's performance.

Comparative Analysis: The variations in thrust and specific impulse were compared across all grain sizes, validating the accuracy of the numerical simulations.

The results demonstrate the effectiveness of flow simulation in predicting SRM performance and provide a foundation for optimizing future designs.

4 Validation of Results

To ensure the accuracy and reliability of the simulated results, a validation process was conducted by comparing the CFD simulation outputs with theoretical values obtained from an isentropic aerodynamic calculator or isentropic relations.This approach helps assess the consistency of the numerical model with well-established analytical solutions.

CALCULATIONS FROM ISENTROPIC RELATIONS

Table 5: Table of isentropic relation values

Where,

x – Length of the iso-surface from the throat, r – Radius of the iso-surface,A/At - Area ratio, M – Mach Number, T/To – Ratio of static temperature to the total temperature, T/T* - Ratio of static temperature to the temperature at throat, P/Po – Ratio of static pressure to the total pressure, P/P* - Ratio of static pressure to the preessure at the throat.

Calculations from CFD Simulations

x	**r**	**A/At**	**M**	**T/To**	**T/T***	**P/Po**	**P/P***
0.01	0.01659	1.223	1.565	0.6711	0.8053	0.2476	0.4688
0.02	0.01928	1.6520	1.974	0.5619	0.6743	0.1330	0.2517
0.03	0.02196	2.143	2.274	0.4914	0.5897	0.0832	0.1575
0.04	0.02464	2.698	2.524	0.4396	0.5275	0.0563	0.1066
0.05	0.02732	3.317	2.743	0.3991	0.4789	0.00401	0.0760
0.06	0.030	4	2.9401	0.3664	0.4397	0.02978	0.0563
0.07	0.03269	4.749	3.1206	0.3392	0.4071	0.0227	0.0430
0.08	0.03537	5.56	3.286	0.3163	0.3796	0.0178	0.0337
0.09	0.03805	6.434	3.442	0.2967	0.3560	0.0142	0.0269
0.1	0.04341	8.375	3.727	0.2646	0.3175	0.0095	0.0180
x	r	A/At	M	T/To	T/T*	P/Po	P/P*
0.01	0.01659	1.223	1.513	0.686	0.823	0.264	0.446
0.02	0.01928	1.6520	1.896	0.582	0.6982	0.144	0.2469
0.03	0.02196	2.143	2.211	0.506	0.6072	0.0865	0.164
0.04	0.02464	2.698	2.43	0.458	0.550	0.0599	0.1138
0.05	0.02732	3.317	2.63	0.421	0.5057	0.0435	0.0827
0.06	0.030	4	2.81	0.388	0.4413	0.0315	0.060
0.07	0.03269	4.749	2.96	0.3651	0.437	0.0246	0.0467
0.08	0.03537	5.56	3.173	0.345	0.413	0.0186	0.0373
0.09	0.03805	6.434	3.394	0.3012	0.3741	0.0155	0.0294

0.1	0.04341	8.375	3.671	0.2841	0.3389	0.0107	0.0204

Table 6: Table of CFD simulation values

ISENTROPIC RELATIONS VS CFD SIMULATION GRAPHS

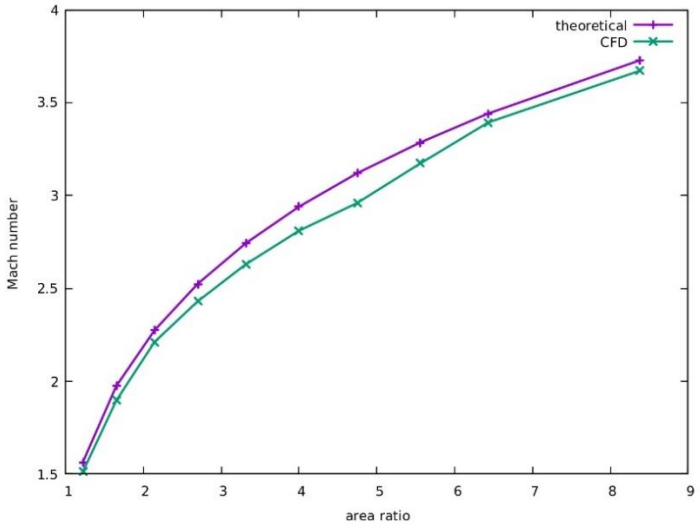

Figure 12: MACH NUMBER VS AREA RATIO (M VS A/AT)

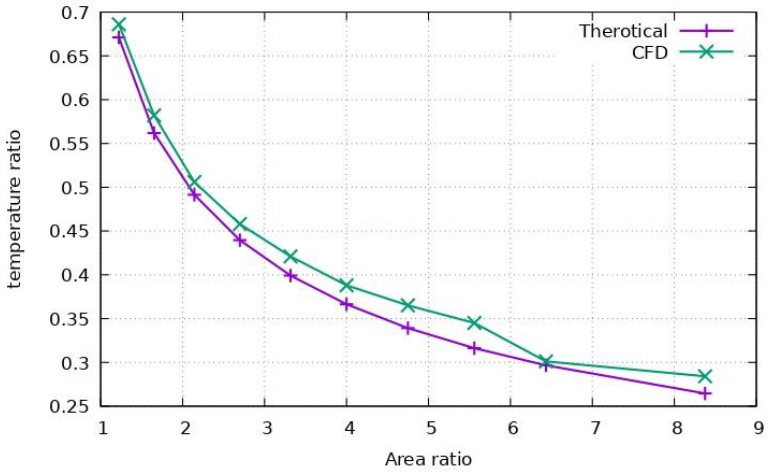

Figure 13: TEMPERATURE RATIO VS AREA RATIO (T/TO VS A/AT)

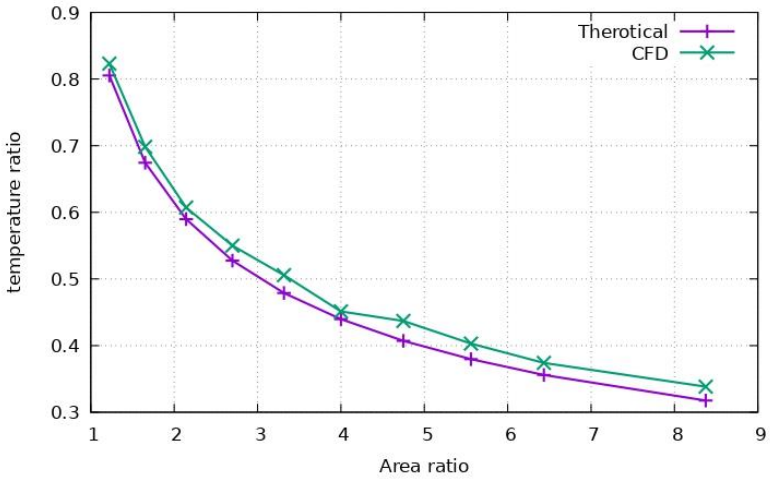

Figure 14: TEMPERATURE RATIO VS AREA RATIO (T/T* VS A/AT)

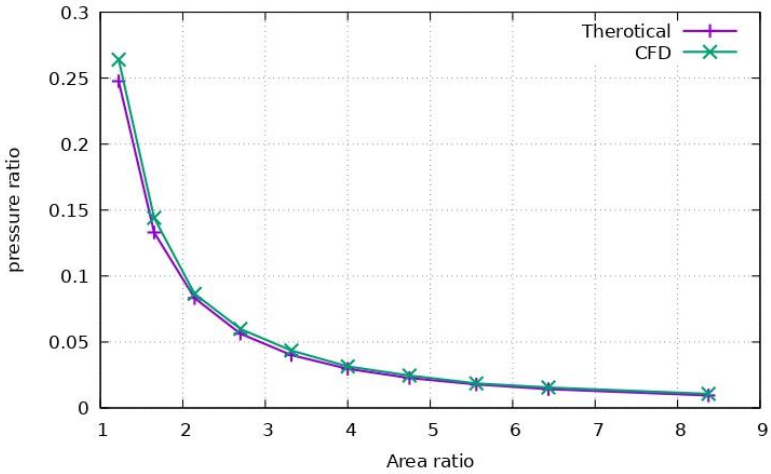

Figure 15: PRESSURE RATIO VS AREA RATIO (P/PO VS A/AT)

The validation confirms that the simulation results align well with theoretical predictions, with acceptable discrepancies due to real-world aerodynamic effects. This ensures that the numerical approach used for flow simulation is reliable for further analysis of the solid rocket motor.

4. Conclusion

This study presents a CFD-based approach for analyzing the internal flow behavior and thrust characteristics of a solid rocket motor with a tubular grain configuration. The simulation model accurately reflects the burnback process by progressively reducing grain length and capturing the corresponding changes in flow parameters. The results show a clear and consistent reduction in thrust as the grain regresses, confirming the relationship between burning surface area and motor performance. Mach number distribution, pressure, and temperature fields align with theoretical expectations, and validation against isentropic flow data confirms the model's reliability. The project concludes that CFD is an effective and practical tool for predicting SRM performance, offering valuable insights for design and optimization.

6 References

1. G. P. Sutton and O. Biblarz, Rocket Propulsion Elements, 8th ed. Hoboken, NJ, USA: Wiley, 2010.

2. P. Hill and C. Peterson, Mechanics and Thermodynamics of Propulsion, 2nd ed. Reading, MA, USA: Addison-Wesley, 1992.
3. D. K. Huzel and D. H. Huang, Modern Engineering for Design of Liquid Propellant Rocket Engines. Reston, VA, USA: AIAA, 1992.
4. G. V. R. Rao, "Exhaust nozzle contours for optimum thrust," Jet Propulsion, vol. 28, no. 6, pp. 377–382, 1958.
5. A. Khawaji, et al., "CFD simulation of flow through convergent-divergent nozzles," Journal of Mechanical Science and Technology, vol. 31, no. 12, pp. 5921–5927, 2017.
6. S. Ghosh and A. Majumdar, "CFD analysis of solid rocket motor internal flow," Aerospace Science and Technology, vol. 27, no. 1, pp. 305–314, 2013.
7. V. Yang, T. B. Brill, and W. Z. Ren, Eds., Solid Propellant Chemistry, Combustion, and Motor Interior Ballistics, vol. 185, AIAA Progress in Astronautics and Aeronautics, 2000.
8. K. P. Sudheer and G. Gopalakrishna, "CFD analysis of solid rocket motor nozzle," International Journal of Aerospace and Mechanical Engineering, vol. 9, no. 1, pp. 25–30, 2015.
9. T. P. Rao, et al., "Numerical simulation of nozzle flow for various area ratios," International Journal of Engineering Research and Applications, vol. 6, no. 3, pp. 35–42, 2016.
10. R. Nakka, "Solid Propellant Rocket Fundamentals," 2003. [Online]. Available: http://www.nakka-rocketry.net/
11. A. B. Gohil and B. M. Panchal, "CFD analysis of convergent-divergent nozzle using Ansys Fluent," International Journal for Research in Applied Science & Engineering Technology (IJRASET), vol. 6, no. 5, pp. 877–884, 2018.
12. K. Kaladhar and B. N. Raghunandan, "Grain regression studies in solid rocket motors using CFD," Journal of Propulsion and Power, vol. 27, no. 6, pp. 1321–1328, 2011.
13. J. D. Anderson, Fundamentals of Aerodynamics, 4th ed. New York, NY, USA: McGraw-Hill, 2001.
14. ANSYS Inc., ANSYS Fluent Theory Guide. Canonsburg, PA, USA, 2022.
15. D. James, "CFD simulations of rocket nozzles for different pressure ratios," Aerospace Engineering Journal, vol. 46, no. 3, pp. 211–219, 2009.
16. A. Garg and V. Sharma, "Analysis of thrust variation with grain geometry in SRMs," International Journal of Engineering and Advanced Technology, vol. 9, no. 4, pp. 451–456, 2020.
17. H. K. Chelliah and V. Yang, "Combustion modeling of solid propellants in rocket motors," Combustion Science and Technology, vol. 87, no. 1, pp. 227–248, 1993.